A numerical investigation of the cracking behaviour of reinforced-concrete tie elements

Tan, Reignard; Hendriks, Max A.N.; Geiker, Mette; Kanstad, Terje

DOI
10.1680/jmacr.18.00156

Publication date
2020

Document Version
Final published version

Published in
Magazine of Concrete Research

Citation (APA)
Tan, R., Hendriks, M. A. N., Geiker, M., & Kanstad, T. (2020). A numerical investigation of the cracking behaviour of reinforced-concrete tie elements. *Magazine of Concrete Research*, *72*(3), 109-121. https://doi.org/10.1680/jmacr.18.00156

Cite this article
Tan R, Hendriks MAN, Geiker M and Kanstad T (2020)
A numerical investigation of the cracking behaviour of reinforced-concrete tie elements.
Magazine of Concrete Research **72(3)**: 109–121,
https://doi.org/10.1680/jmacr.18.00156

Research Article
Paper 1800156
Received 26/03/2018; Revised 25/07/2018;
Accepted 28/08/2018;
Published online 10/10/2018

Keywords: bond/cracks & cracking/finite element methods

Magazine of Concrete Research

ice Publishing

A numerical investigation of the cracking behaviour of reinforced-concrete tie elements

Reignard Tan
PhD candidate, Department of Structural Engineering, Norwegian University of Science and Technology, Trondheim, Norway (corresponding author: reignard.tan@multiconsult.no) (Orcid:0000-0001-8190-6215)

Max A. N. Hendriks
Professor, Department of Structural Engineering, Norwegian University of Science and Technology, Trondheim, Norway; Faculty of Civil Engineering and Geosciences, Delft University of Technology, Delft, the Netherlands (Orcid:0000-0001-9507-3736)

Mette Geiker
Professor, Department of Structural Engineering, Norwegian University of Science and Technology, Trondheim, Norway (Orcid:0000-0003-4952-8394)

Terje Kanstad
Professor, Department of Structural Engineering, Norwegian University of Science and Technology, Trondheim, Norway (Orcid:0000-0003-0760-2322)

The cracking behaviours of reinforced-concrete (RC) ties are investigated by conducting virtual experiments using non-linear finite-element analysis. The assumptions in the model are verified by benchmarking the classical experiments of B. Bresler and V. V. Bertero as conducted in 1968 and P. J. Yannopoulos, conducted in 1989, which shows good agreement in the comparison of steel strains, development of crack widths and crack spacing. Furthermore, virtual experiments on four different RC ties show that the size of the cover and not the bar diameter governs the crack spacing and thus implicitly the crack width. An increase of the bar diameter has a beneficial effect in reducing the steel stress and the associated steel strains, which in turn reduces the crack width. Finally, a single bond–slip curve is sufficient in describing the average bond transfer of an arbitrary RC tie.

Notation

A_c	area of concrete
A_s	area of steel
c	cover
E_c	modulus of elasticity of concrete
E_s	modulus of elasticity of steel
F_c	force resultant of concrete
F_{cr}	cracking force of concrete
f_c	compressive strength of concrete
f_{ct}	tensile strength of concrete
f_y	yield strength of steel
G_f	tensile fracture energy of concrete
G_{fc}	compressive fracture energy of concrete
L	bar length
N	applied force at steel bar ends
R	radial axis
s	slip
s_1	slip parameter in bond–slip curve according to *fib* Model Code 2010
s_r	specific distance from the loaded end
t_i	thickness of interface layer between concrete and steel
w_i	crack width at the steel bar surface
w_o	crack width at the specimen surface
x	position over the bar length
x_{cr}	crack spacing
x_i	x-coordinate of integration points adjacent to the steel and outer concrete surface
x_r	transfer length
α	curve parameter in bond–slip curve according to *fib* Model Code 2010
Δx	half finite-element length
ε_c	strains at outer concrete surface
ε_{ci}	concrete strains at integration points
ε_{ct}	cracking strain concrete
ε_s	strains at steel surface
ε_{si}	steel strains at integration points
ν_c	Poisson ratio of concrete
ν_s	Poisson ratio of steel
ρ_{eff}	reinforcement ratio
σ_s	steel stress
τ_1	bond stress parameter in bond–slip curve according to *fib* Model Code 2010
$\tau_{bm,x_{cr}}$	mean bond stress over the crack distance
ϕ	bar diameter

Introduction

In deriving an analytical crack width calculation model for reinforced-concrete (RC) elements, the roles of (*a*) bond at the steel–concrete interface and (*b*) cover become two key parameters (Balázs *et al.*, 2013; CEB, 1985). This paper investigates these two parameters using non-linear finite-element (FE) analyses (NLFEA), which were validated against classical experiments. The tensile strength of concrete is a third key parameter. This parameter has been investigated thoroughly in the research project of CEOS.fr (Barre *et al.*, 2016), in which the scale effect is accounted for in determining the concrete tensile strength, and will not be addressed in detail here.

The roles of bond and cover are implemented in the empirical formulation recommended by the American Concrete Institute (ACI, 2001) and in the semi-empirical formulation recommended by Eurocode 2 (CEN, 2004) and *fib* Model Code 2010 (MC2010) (*fib*, 2013) in a relatively simplified manner. The bond and cover terms in the crack spacing formula of

Eurocode 2 and MC2010 are based on two different mechanical models and are as such in conflict with the basic principles in statics (Tan *et al.*, 2018). The authors in this paper claim that a more mechanically consistent crack width calculation model can be formulated by including the two key parameters in deriving and solving the second-order differential equation for the slip. In such an analytical model, the choice of a local bond–slip curve becomes essential. Although the relevance of a local bond–slip curve is well understood for pull-out tests (*fib*, 2000), this seems not to be the case for RC ties subjected to pure tension. Although several authors have contributed to the discussions by conducting experiments on concentric tension specimens (Dörr, 1978; Jiang *et al.*, 1984; Mirza and Houde, 1979; Nilson, 1972; Somayaji and Shah, 1981), the answer to the question of what a local bond–slip model physically represents in an RC tie subjected to pure tension still remains unclear. There seems to be a consensus in the literature (Balázs, 1993; Debernardi and Taliano, 2013, 2016; Russo and Romano, 1992) in choosing the local bond–slip model proposed by Eligehausen *et al.* (1983) and later adopted by MC2010. The parameters involved, however, were determined empirically based on pull-out tests in which the confining concrete was subjected to compression. The problem thus becomes related to choosing proper values that are representative in the case of RC ties subjected to pure tension.

In this study, the authors seek to contribute to a better understanding of the cracking behaviour of RC ties with deformed steel bars subjected to pure tension by conducting virtual experiments using NLFEA. Such virtual experiments offer the possibility of monitoring the internal behaviour of the confining concrete, a convenience that is often limited in physical experiments. First, important assumptions in the FE model are discussed. Second, the classical experiments of Bresler and Bertero (1968) and Yannopoulos (1989) are benchmarked to investigate the validity of the assumptions in the FE model and the cracking behaviour of RC ties. Then, the roles of bar diameter and cover are investigated and discussed by conducting virtual experiments on four different RC ties. Finally, values for the parameters in the local bond–slip curve recommended by MC2010 (*fib*, 2013) are proposed. These can be used in an analytical crack width calculation model after having solved the second-order differential equation for the slip. The authors in this paper are currently working on such an approach.

Finite-element model

Main assumptions

Detailed NLFEA of RC ties with small element sizes (<10 mm) are normally carried out using interface elements between concrete and steel – for example, as suggested by Lutz (1970) and conducted by Tammo *et al.* (2009). This can be useful to account for effects such as the wedging action between the bar ribs and the surrounding concrete without physically modelling the geometry of the bar ribs, as well as accounting for the effect of slip when adhesion breaks down. In this study, interface elements are used to allow for separation but not any slip, meaning that the concrete at the interface is assumed to follow the longitudinal displacement field of steel completely. This further implies that the bond transfer at the interface is mechanically maintained, although the concrete is separated radially from the steel bar. This assumption is based on the experimental behaviour of RC ties reported in the literature, in which there is a general agreement that the crack width at the steel bar surface is significantly smaller than that on the concrete surface in the case of deformed steel bars (Beeby, 2004; Borosnyói and Snóbli, 2010; Broms, 1968; Husain and Ferguson, 1968; Watstein and Mathey, 1959; Yannopoulos, 1989). The research of Goto (1971) and Tammo and Thelandersson (2009) concludes that this occurs due to the rib interaction between concrete and steel, which causes the concrete to crack internally, thus allowing it to follow the longitudinal displacement field of steel at the interface, as depicted in Figure 1(a).

Note that the assumption of neglecting the crack width at the steel bar surface allows the use of a relatively simple FE model, in which shear deformations in the steel concrete interface are prohibited and the explicit modelling of the bar ribs is avoided. This means that localised bond stresses that would arise at the bar ribs are smeared over the rebar. This also implies that effects related to the rib geometry or other bond conditions – for example, wedging action or slip due to loss of adhesion – cannot be captured in this FE model. These effects, however, normally remain limited in RC ties with deformed steel bars subjected to pure tension (*fib*, 2000), making the simple FE model adequate for the purpose of this study.

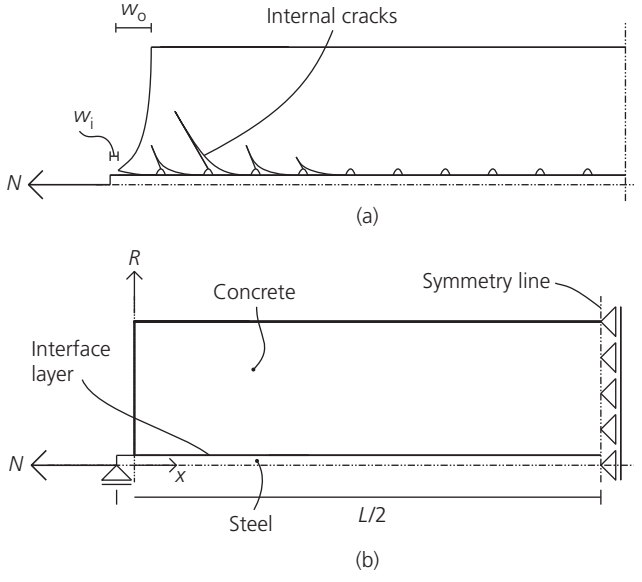

Figure 1. (a) Typical deformation configuration of RC ties with deformed steel bars; (b) FE model

Axisymmetric model

The NLFEA were carried out using quadratic, axisymmetric, quadrilateral elements in the FE program 'Diana' (Diana FEA BV, 2016). A linear elastic material model was used for steel, while a non-linear fracture mechanics material model with rotating cracks based on a total strains formulation was used for concrete. The parabolic curve according to Feenstra (1993) was used for the compressive behaviour, whereas the softening curve according to Hordijk (1991) was used for the tensile behaviour. The Poisson effect was gradually reduced in accordance with the total strains formulation as the cracking damage progressed, while lateral influences on the compressive behaviour were neglected. Geometry, interface layer, loading and boundary conditions for the FE model are as shown in Figure 1(b). Symmetry allowed for modelling half of the length only.

Loads were monotonically increased in a displacement-controlled manner using regular Newton–Raphson iterations. The convergence criteria were force and energy based with the tolerance value of 0·01 and 0·001, respectively, in accordance with the Dutch guidelines for NLFEA of concrete structures (Belletti *et al*., 2014; Hendriks *et al*., 2017). The element size was adjusted to obtain approximately six to ten elements over the cover and one to three elements over the steel bar radius.

Interface elements between concrete and steel were chosen to have a thickness of $t_i = 0{\cdot}1$ mm. A non-linear elasticity model with non-linear properties in the radial direction and a constant stiffness in the shear direction were chosen to allow for radial separation only in accordance with the assumptions discussed in the previous section. The elastic radial and shear moduli for the interface elements were derived from the modulus of elasticity for concrete, E_c – that is, respectively, as E_c/t_i and $E_c/[2(1+v_c)t_i]$. The elastic radial modulus was reduced with a factor of 10^{-05} when a tensile strain of $0{\cdot}8f_{ct}/E_c$ at the interface was reached, in order to simulate the radial separation in a stable manner.

Validation of FE model

Test set-up

The classical experiments of Bresler and Bertero (1968) and Yannopoulos (1989) were benchmarked to investigate the validity of the assumptions in the FE model. The investigated RC tie named specimen H by Bresler and Bertero (1968) was 152 mm (6 in) in diameter, had a length of 406 mm (16 in) and was embedded with a deformed steel bar with dia. 28·7 mm (1·13 in) in the centre of the cross-section. The length of the specimen was chosen as twice the mean crack spacing obtained from the pilot studies of 1829 mm (72 in) long RC ties with similar sectional properties. The specimen was axially cyclic loaded in the steel bar ends in the experiments, and a notch was cut at the mid-length to induce a primary crack at this section. Strain gauges were mounted in a sawed-out canal in the centre of the steel bar to measure the steel strains over the length. The reduction of the steel bar area due to the sawed-out canal was accounted for by subtracting an inner radius of 5·6 mm from the outer radius of the steel bar in the FE model. This corresponded to the given nominal area of 548 mm^2 (0·85 in^2) for the steel bar in the experiments.

The six RC ties investigated by Yannopoulos (1989) were 76 mm in diameter, had a length of 100 mm and were embedded with a deformed steel bar of dia. 16 mm in the centre of the cross-sections. The length of the specimens was limited to avoid formation of a new primary crack and was based on the mean crack spacing obtained from pilot studies carried out on 800 mm long RC ties with similar sectional properties. The RC ties were axially and monotonically loaded at the steel bar ends while measuring the development of the crack width.

The material parameters given in the experiments are summarised in Table 1 and were used in validating the FE model. Material parameters such as the Poisson ratio and the fracture energy were not given in the experiments and were derived in accordance with the recommendations in the Dutch guidelines for NLFEA of concrete structures (Hendriks *et al*., 2017).

Comparison of steel strains, crack widths and crack spacing

The comparison of the steel strains obtained from the NLFEA and the experimental steel strains of Bresler and Bertero (1968) at four different load levels is shown in Figure 2(a). The two lowest load levels corresponding to steel stresses of 33 MPa and 65 MPa give good comparisons of the steel strains, as expected, since the experimental strains at these load levels are obtained from the first monotonic load cycle. The experimental strains at the two higher load levels corresponding to steel stresses of 195 MPa and 242 MPa, however, are obtained from the second load cycle. Cyclic loading is known to have a significant effect on the deterioration of bond even for the first repeated loads (Dörr, 1978; *fib*, 2000), which could explain the less stiff response of the experimental steel strains in the second load cycle compared to that obtained from the monotonic loading in the NLFEA. Nevertheless, the comparison of the steel strains obtained from the NLFEA and the experiments shows in general a good agreement.

A comparison of the development of the crack width with increasing steel stresses obtained in the experiments of Yannopoulos (1989) and in the NLFEA is shown in Figure 2(b). The comparison of the developed crack width also shows good agreement; however, it is observed that the NLFEA slightly overestimates the crack width for a given steel stress.

Separate NLFEA were conducted to investigate whether the FE model also could predict crack spacing similar to that

Table 1. Material parameters of the RC ties investigated in the experiments of Bresler and Bertero (1968) and Yannopoulos (1989)

	Bresler and Bertero (1968)		Yannopoulos (1989)	
Material parameters	Concrete	Steel	Concrete	Steel
Compressive strength, f_c: MPa	40·8	—	43·4	—
Tensile strength, f_{ct}: MPa	4·48	—	3·30	—
Yield strength, f_y: MPa	—	413	—	424
Modulus of elasticity, E_c and E_s: MPa	33 165	205 464	32 000	200 000
Poisson ratio, ν_c and ν_s	0·15	0·30	0·15	0·30
Tensile fracture energy, $G_f = \frac{73 f_c^{0.18}}{1000}$: N/mm	0·142	—	0·144	—
Compressive fracture energy, $G_c = 250 G_f$: N/mm	35·6	—	36·0	—

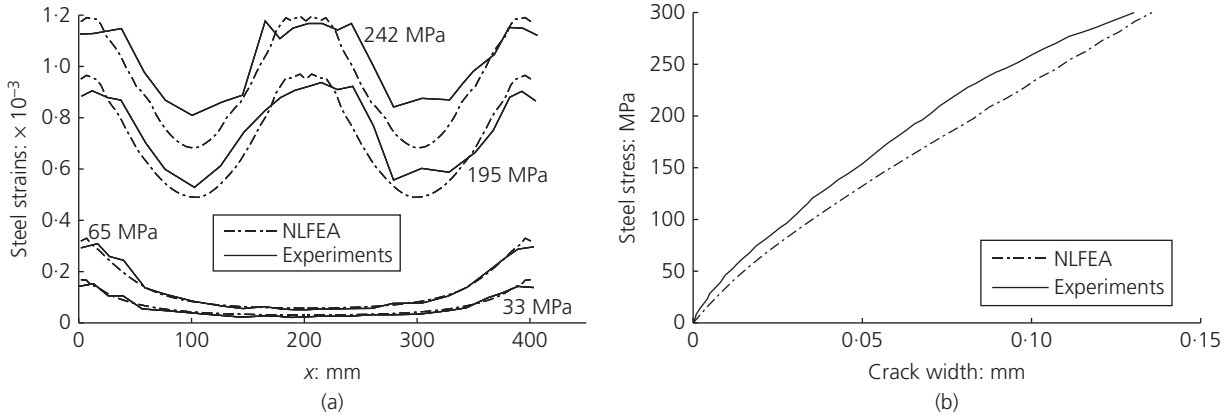

Figure 2. (a) Comparison of steel strains in the experiments of Bresler and Bertero (1968) with steel strains obtained in the NLFEA. (b) Comparison of crack widths in the experiments of Yannopoulos (1989) with crack widths obtained in the NLFEA

obtained in the pilot studies of Bresler and Bertero (1968) and Yannopoulos (1989) on longer specimens. The RC tie lengths were thus increased in the FE model to investigate this. The strain distribution in Figures 3(a) and 3(b), respectively, shows that a new crack formed in the NLFEA at a distance of approximately 200 mm from the loaded end for the long 'Bresler and Bertero' specimen and at approximately 80 mm for the long 'Yannopoulos' specimen. This corresponds well to the mean crack spacing of 203 mm and 90 mm, respectively, obtained in the experiments of Bresler and Bertero (1968) and Yannopoulos (1989) on longer specimens.

The good agreement in the comparison of steel strains, crack widths and crack spacing confirms the validity of the discussed assumptions, and further shows the ability of the FE model to simulate the physical behaviour of RC ties realistically.

The physical behaviour of RC ties

General

The physical behaviour of RC ties is now discussed and elucidated using the results from the NLFEA conducted on the 'Bresler and Bertero' specimen. Details for the test set-up were presented in the section entitled 'Test set-up'. A contour plot of exaggerated radial displacements at a steel stress, $\sigma_s \approx$ 180 MPa, which is just before a primary crack forms at the symmetry section, is shown in Figure 4(a). It is noticed that the concrete is separated radially from the steel bar close to the loaded end due to the inflicted shear stress at the concrete inner surface. The radial displacements are counteracted by the stiffness of the concrete in the hoop direction, causing a confining pressure to the steel bar. Splitting cracks arise if the hoop stresses exceed the tensile strength of concrete, as can be observed in Figure 4(b). Actually, the splitting cracks cause a build-up of radial and shear stresses close to the loaded end, before reaching the peaks at approximately the same location over the bar length, as can be observed in Figure 4(c). Further propagation of internal splitting cracks as the load increases causes additional movement of the stress peaks towards the symmetry section.

It should be mentioned that the maximum radial displacements in the analyses are of the magnitude of 10^{-2} mm, which is still small compared to typical rib dimensions. This justifies the assumption of claiming that the mechanical bond is maintained although the concrete is separated radially from

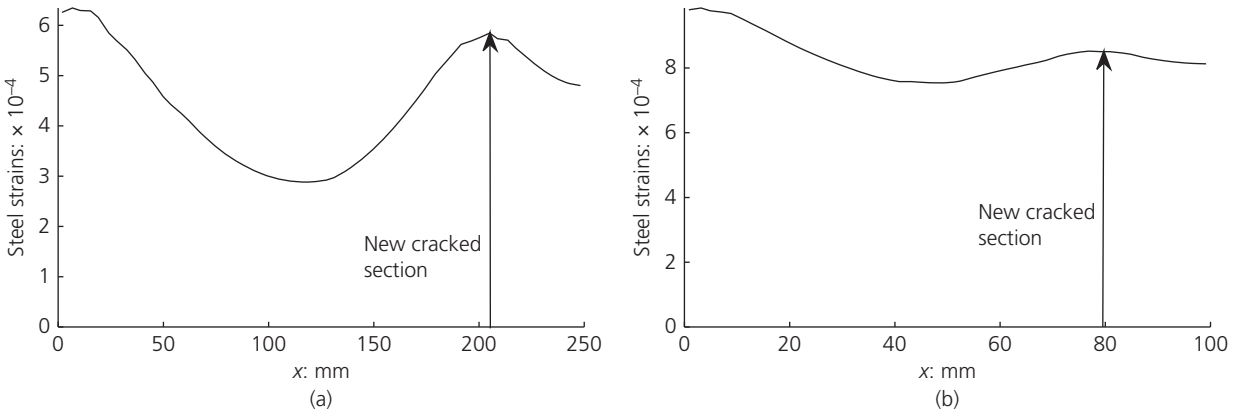

Figure 3. Steel strain distributions obtained from the NLFEA immediately after the formation of a new primary crack for (a) the long 'Bresler and Bertero' specimen ($L = 500$ mm) and (b) the long 'Yannopoulos' specimen ($L = 200$ mm)

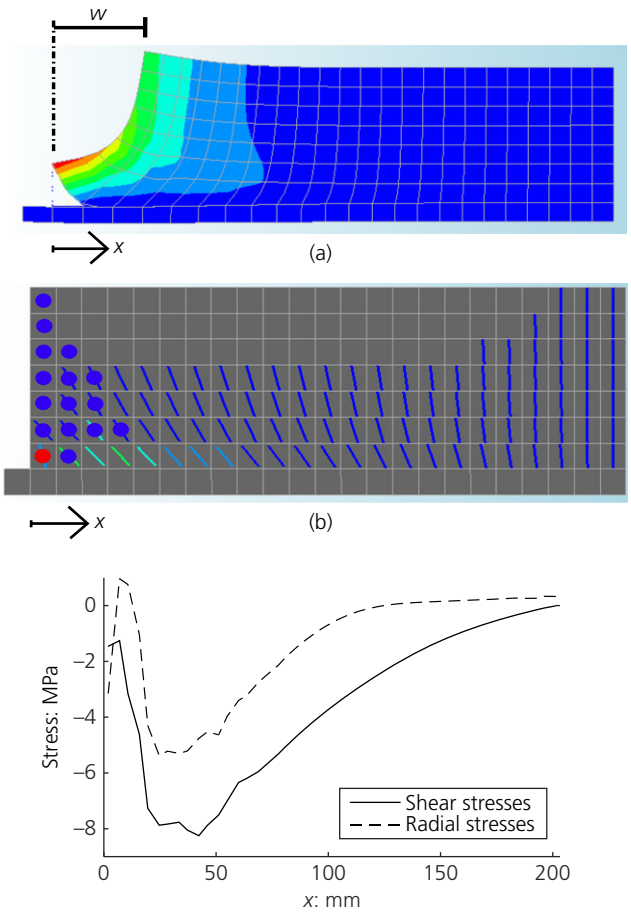

Figure 4. (a) Contour plot of radial displacements and the deformation configuration at $\sigma_s = 180$ MPa. (b) Corresponding plot of internally inclined cracks (straight lines) and splitting cracks (circles). (c) Corresponding shear and radial stresses. A full-colour version of this figure can be found on the ICE Virtual Library (www.icevirtuallibrary.com)

the steel bar. Finally, these observations suggest that the shear transfer is dependent on the stiffness of the confining concrete.

Lightly as opposed to heavily loaded members

The interaction of the load level and the specimen length is significant for the cracking behaviour of RC ties. Russo and Romano (1992) were the first to introduce the principles of the comparatively lightly loaded member (CLLM) behaviour and the comparatively heavily loaded member (CHLM) behaviour, which are conceptually visualised in Figures 5(a) and 5(b), respectively. The figures depict the steel and the corresponding concrete strain distribution of a long specimen with length $L = 500$ mm and a short specimen with length $L = 200$ mm, exposed to the same loading. To clarify, the arrows in Figure 5(b) indicate the corresponding concrete surface strains to the steel strains for the short specimen. The main difference is that the strains become compatible ($\varepsilon_s = \varepsilon_c$) at a certain distance x_r from the loaded end and remain constant along the remaining length in the case of CLLM, whereas in the case of CHLM the strains remain incompatible ($\varepsilon_s > \varepsilon_c$) over the entire specimen length. The point of compatibility x_r moves towards the symmetry section upon increasing the load, and will have moved completely to the symmetry section ($x_r = L/2$) for a sufficiently large load in the case of CLLM. Upon even further loading, strains become incompatible at the symmetry section and a primary crack will only have the possibility to form here if the concrete strains exceed the cracking strain. The specimen can then be said to have undergone a smooth transition from the CLLM behaviour to the CHLM behaviour. If the concrete strains exceed the cracking strain at any location prior to the symmetry section – that is, $\varepsilon_c(x_r) \geq \varepsilon_{ct}$, a new primary crack will instead form here, thus generating a new member length $L = x_r = x_{cr}$. The new member will then exhibit either a CLLM behaviour or a CHLM behaviour depending on the load level and the member length.

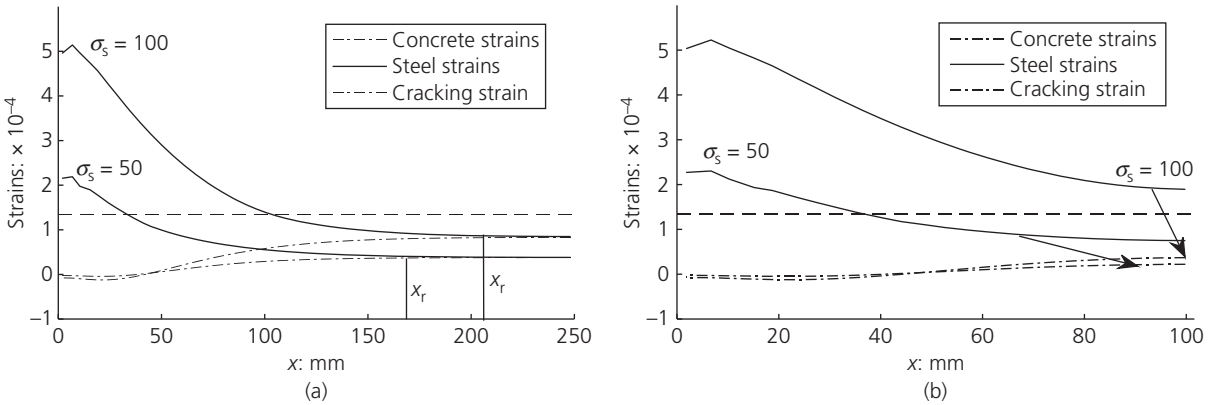

Figure 5. Strain distribution for the 'Bresler and Bertero' specimen at two similar load levels: (a) CLLM behaviour of a long specimen $L = 500$ mm; (b) CHLM behaviour of a short specimen $L = 200$ mm

An analogy of the CLLM and CHLM behaviour can be drawn to the so-called crack formation stage and stabilised cracking stage, respectively. However, they are not the same. This can be explained by the fact that a smooth transition between the CLLM and the CHLM behaviour is possible, which is not the case in the concept of the crack formation stage and stabilised cracking stage.

The influence of bar diameter and cover on the cracking behaviour of RC ties

Virtual experiments

The bar diameter and cover are essential parameters in calculating the crack spacing and the crack width in the semi-empirical formulas recommended by Eurocode 2 (CEN, 2004) and MC2010 (*fib*, 2013). Both parameters have been the subject of major discussions for several decades in developing the semi-empirical formulas (Base *et al.*, 1966; Beeby, 1979, 2004; Broms, 1968; Caldentey *et al.*, 2013; Ferry-Borges, 1966; Gergely and Lutz, 1968; Saliger, 1936; Tan *et al.*, 2018). For this purpose, the FE model established and verified in this study has been used to conduct virtual experiments on RC ties to better understand the influence of bar diameter and cover.

The behaviours of four circular specimens, reinforced with one concentric deformed steel bar, were investigated. The specimens were named $\phi 20c40$, $\phi 20c90$, $\phi 32c40$ and $\phi 32c90$, indicating that the bar diameter ϕ was either 20 or 32 mm and that the cover c was either 40 mm or 90 mm. A concrete grade C35 according to MC2010 (*fib*, 2013) was chosen for the concrete, while a Young's modulus of $E_s = 200\,000$ MPa and a yield strength of $f_y = 500$ MPa was chosen for the steel. The Poisson ratio and the fracture energy were derived in accordance with the recommendations in the Dutch guidelines for NLFEA of concrete structures (Hendriks *et al.*, 2017). The analysis procedure was to first conduct CLLM studies on longer specimens ($L = 700$ mm) to obtain a typical crack spacing x_{cr}, after which a separate analysis on the cracked specimen was conducted to include the CHLM behaviour.

The influence of bar diameter

CLLM behaviour

The bond stress distributions for the CLLM behaviour of $\phi 20c40$ against $\phi 32c40$ and $\phi 20c90$ against $\phi 32c90$ are compared at the load levels just before a primary crack forms in Figures 6(a) and 6(b), respectively, with Table 2 showing the corresponding condition in the specimens. The comparison shows that the bond stress distributions are influenced greatly by the bar diameter and differ in general from one another. It is noticed, however, that the bond stress distributions align and become negligibly small ($\tau < 1$ MPa) at approximately the same location over the bar length, indicating the end of the transfer length and that a primary crack is about to form in the vicinity. The concrete force resultant at a distance s_r from the loaded end is obtained by integrating the bond stress distribution $\tau(x)$ as

$$1. \quad F_c(x_{cr}) = \int_0^{s_r = x_{cr}} \tau(x)\pi\phi \mathrm{d}x = \tau_{bm,x_{cr}}\pi\phi x_{cr}$$

which is limited by the cracking force as

$$2. \quad F_{cr} = f_{ct}A_c$$

Although the bar diameter influences the bond stress distribution and thus the concrete force resultant in Equation 1, it does not significantly affect the limit value in Equation 2, nor does it influence the transfer length as pointed out for Figures 6(a) and 6(b). This means that a primary crack forms at approximately the same location over the bar length for

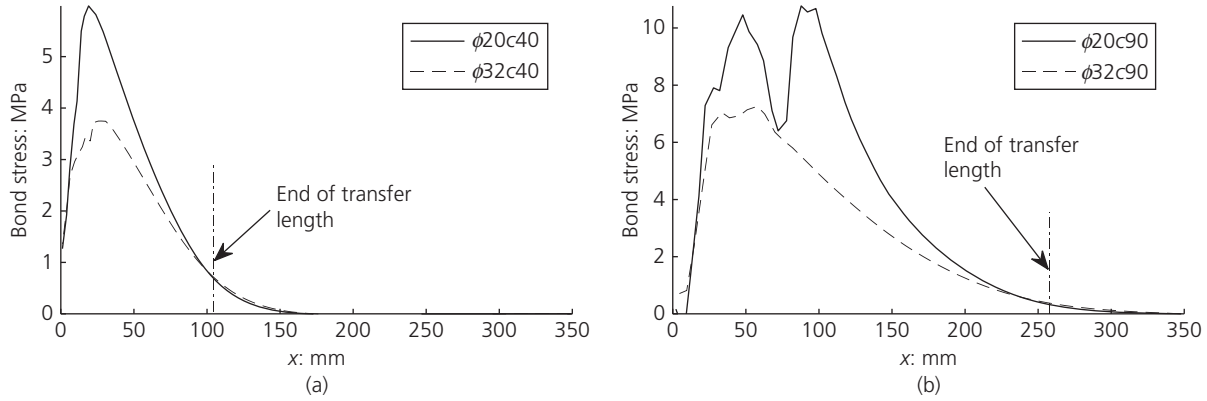

Figure 6. (a) Bond stress distribution for the CLLM behaviour of ϕ20c40 against ϕ32c40 at primary cracking in accordance with the load levels in Table 2. (b) Bond stress distribution for the CLLM behaviour of ϕ20c90 against ϕ32c90 at primary cracking in accordance with the load levels in Table 2

Table 2. CLLM behaviour of ϕ20c40 against ϕ32c40 and ϕ20c90 against ϕ32c90 showing the steel stress σ_s and the corresponding load level F just before a primary crack forms at a distance s_r from the loaded end, mean bond stress $\tau_{bm,x_{cr}}$ of the bond stress distribution over the crack distance x_{cr}, concrete force resultant at the section where a primary crack forms, $F_c(x_{cr}) = \tau_{bm,x_{cr}}\pi\phi x_{cr}$, and the cracking force, $F_{cr} = f_{ct}A_c$

RC tie	σ_s: MPa	F: kN	x_{cr}: mm	$\tau_{bm,x_{cr}}$: MPa	$F_c(x_{cr})$: kN	F_{cr}: kN
ϕ20c40	100·3	31·5	105	3·76	24·8	24·2
ϕ32c40	58·1	46·7	109	2·74	30·0	29·0
ϕ20c90	341·1	107·1	260	6·23	101·8	99·8
ϕ32c90	160·6	129·1	272	4·21	115·1	110·7

specimens having similar cover, irrespective of the bar diameter size, as also can be observed in Table 2.

CHLM behaviour

The strain distribution for the CHLM behaviour of ϕ20c40 against ϕ32c40 and ϕ20c90 against ϕ32c90 with specimen lengths similar to the crack spacing in Table 2 is shown in Figures 7(a) and 7(b), respectively, at two steel stress levels, while the development of the crack width with steel stresses is shown in Figures 7(c) and 7(d). It is observed that the bar diameter influences the strain distribution over the bar length for a given steel stress. The 20 mm specimens experience more variation in steel strains than the 32 mm specimens. This can be explained by the fact that the 32 mm specimens are exposed to a substantially higher load level than the 20 mm specimens for a given steel stress. This implies that the confining concrete for the 32 mm specimens is exposed to more internal cracking than the 20 mm specimens, which has a significant limiting effect on the tension stiffening. Less tension stiffening results in a larger crack width for a given steel stress, as can be observed in Figures 7(c) and 7(d), which can be explained by the following. The crack width is obtained by integrating the difference in steel strains and concrete strains at the specimen surface over the bar length as

$$w = \int_0^{x_{cr}} (\varepsilon_s - \varepsilon_c)\mathrm{d}x \quad (3)$$

Acknowledging from Figures 7(a) and 7(b) that the concrete strains are negligible in the case of CHLM behaviour suggests that the major contribution to the crack width must be the steel strains. Hence, a larger reduction in steel strains over the specimen length results in smaller crack width. It should be mentioned, however, that large bar diameters have a beneficial effect in reducing the steel stress and the associated steel strains for a given load level, which in turn reduces the crack width.

The influence of cover

CLLM behaviour

The bond stress distributions for the CLLM behaviour of ϕ20c40 against ϕ20c90 and ϕ32c40 against ϕ32c90 are compared in Figures 8(a) and 8(b), respectively, at two different conditions, one at a similar load level ($\sigma_s \approx 50$ MPa and $\sigma_s \approx 35$ MPa) and the other corresponding to the load levels in Table 2, which is just before a primary crack forms. The comparison of the bond stress distributions at the similar load level shows that they are quite similar, implying that the cover size does not affect the bond transfer significantly for a given load level and bar diameter in the case of CLLM behaviour. However, comparing the bond stress distributions at the load levels just before a primary crack forms shows that both bond stresses and transfer lengths increase with increasing load level and cover, which can be explained mechanically by the following. A larger cover increases the cracking force in accordance

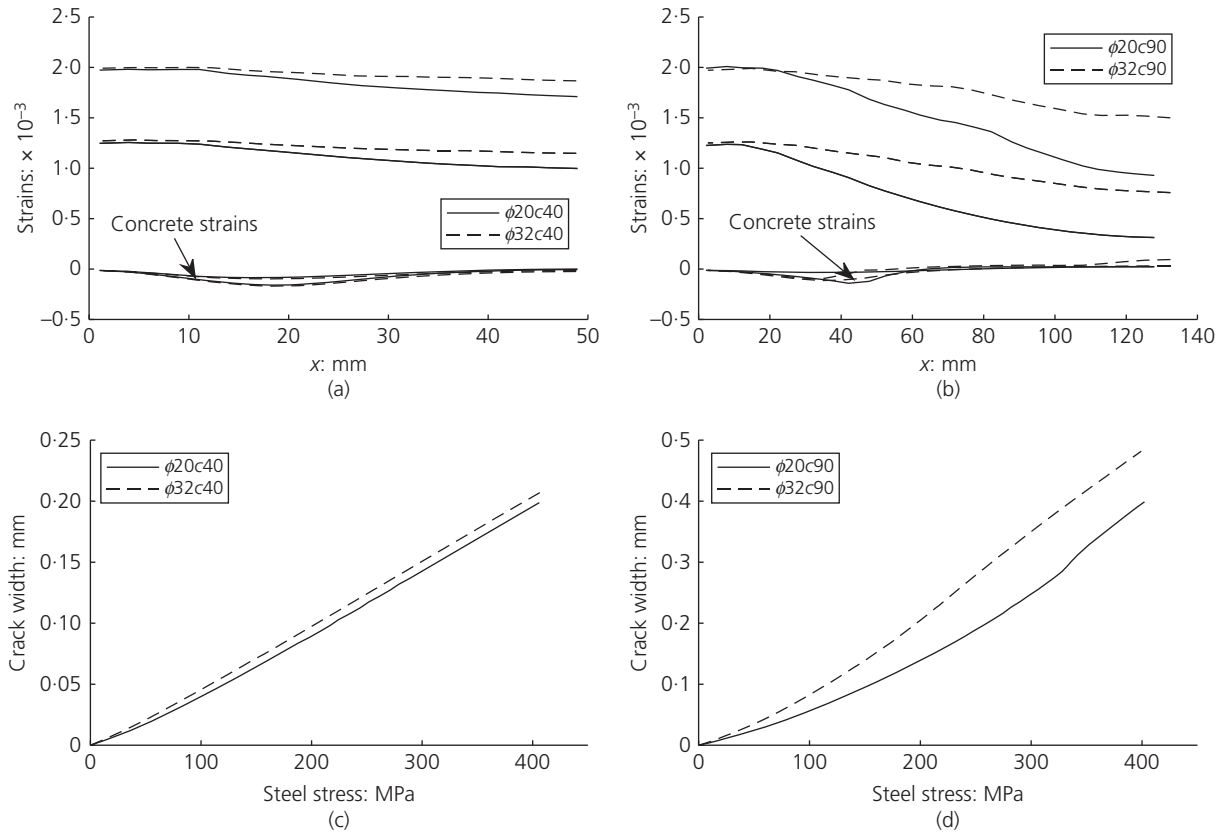

Figure 7. Strain distributions for (a) ϕ20c40 against ϕ32c40 and (b) ϕ20c90 against ϕ32c90 at steel stresses σ_s = 250 MPa and σ_s = 400 MPa. Development of crack widths with steel stresses for (c) ϕ20c40 against ϕ32c40 and (d) ϕ20c90 against ϕ32c90

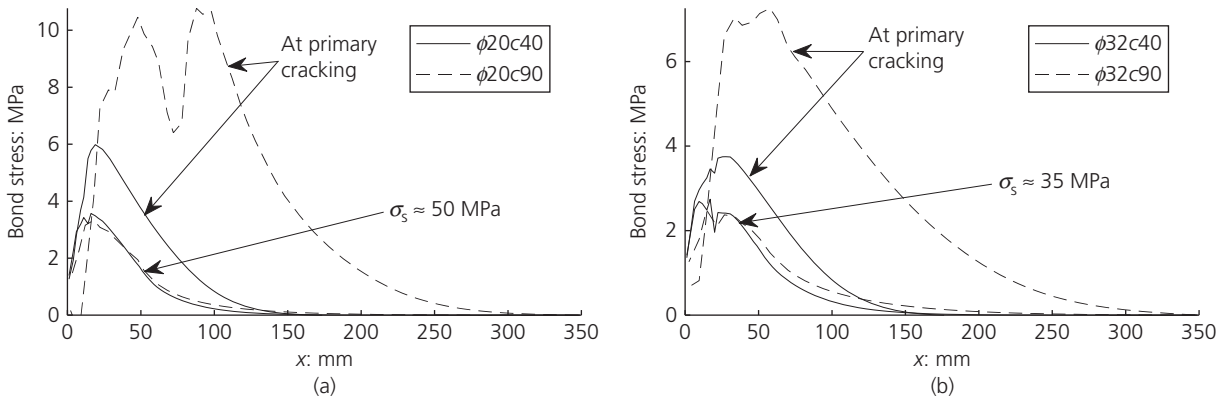

Figure 8. (a) Bond stress distribution for the CLLM behaviour of ϕ20c40 against ϕ20c90 at $\sigma_s \approx 50$ MPa and at primary cracking in accordance with the load levels in Table 2. (b) Bond stress distribution for the CLLM behaviour of ϕ32c40 against ϕ32c90 at $\sigma_s \approx 35$ MPa and at primary cracking in accordance with the load levels in Table 2

with Equation 2. The concrete force resultants, in accordance with Equation 1, however, remain approximately the same at the load level just before a primary crack forms in the specimen having a smaller cover, as the bond stress distributions should be quite similar for a given load level. This means that the concrete force resultant for the specimen having a larger cover can only increase and approach its cracking force by increasing the load level. This in turn results in a larger bond

stress distribution and transfer length, which can also be observed in Table 2 by comparing mean bond stresses and crack spacing for specimens having similar bar diameter but different covers.

CHLM behaviour

The strain distribution for the CHLM behaviour of $\phi 20c40$ against $\phi 20c90$ and $\phi 32c40$ against $\phi 32c90$ with specimen lengths similar to the crack spacing in Table 2 is shown in Figures 9(a) and 9(b), while the development of the crack width with steel stresses is shown in Figures 9(c) and 9(d). The specimens $\phi 20c90'$ and $\phi 32c90'$ are included to represent the hypothetical case in which $\phi 20c90$ and $\phi 32c90$, respectively, were supposed to have the same specimen lengths as $\phi 20c40$ and $\phi 32c40$. It is noticed that the variation in steel strains and the development of crack width nearly remains the same for specimens having similar lengths and bar diameters but different covers. This means that it is the specimen length over which the steel strains are integrated that governs the crack width and not necessarily the cover itself. Hence, the cover does not explicitly influence the crack width per se, but contributes implicitly by increasing the crack spacing. Larger crack spacing simply results in larger crack width, as indicated in Figures 9(c) and 9(d).

The influence of bar diameter and cover on the crack spacing

The discussions regarding Figures 6(a) and 6(b) and Figures 8(a) and 8(b) suggest that the crack spacing is a geometrically dependent parameter, which is mainly governed by the size of the cover but not the bar diameter. A comparable conclusion was drawn by Broms (1968), Gergely and Lutz (1968), Beeby (2004) and Tan *et al*. (2018), primarily by discussing the limited influence of ϕ/ρ_{eff} on the development of crack widths observed in several published experiments. A mechanical explanation of this finding is that the concentrated forces inflicted at the steel bar ends at the moment of cracking, $F = \varepsilon_{\text{ct}}(E_{\text{s}}A_{\text{s}} + E_{\text{c}}A_{\text{c}}) \approx f_{\text{ct}}A_{\text{c}}$, should be close for two specimens having similar cover but different bar diameters since the concrete area A_{c} remains almost the same as discussed earlier, see Table 2. This means that the concentrated forces inflicted at the steel bar ends should disperse in a similar fashion over the cover to obtain an even distribution of the stresses over the cross-section, further implying that the transfer lengths should also be close. Figure 10(a), which shows how the concrete force resultants gradually increase from the loaded end at the load levels corresponding to Table 2, supports this postulation. Further supporting evidence can be observed in Figure 10(b), which shows the development

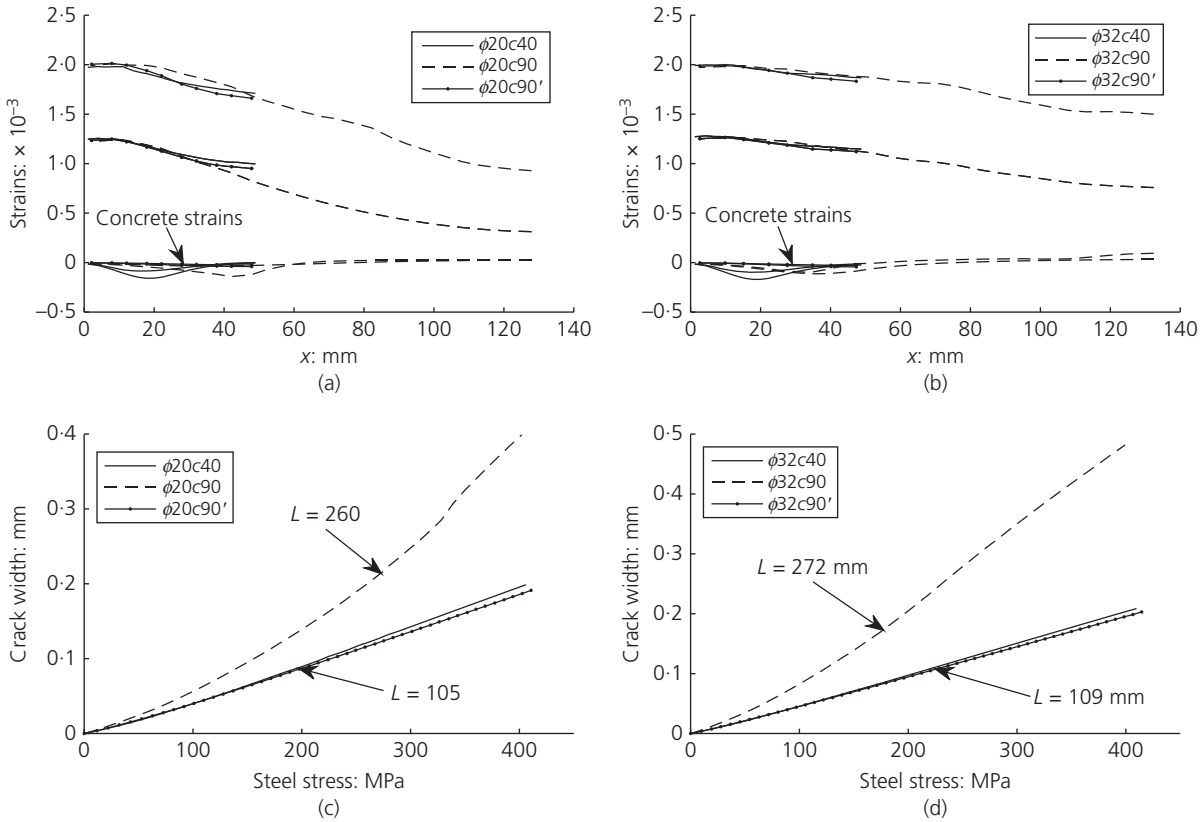

Figure 9. Strain distributions for (a) ϕ20c40 against ϕ20c90 and (b) ϕ32c40 against ϕ32c90. Development of crack widths with steel stresses for (c) ϕ20c40 against ϕ20c90 and (d) ϕ32c40 against ϕ32c90.

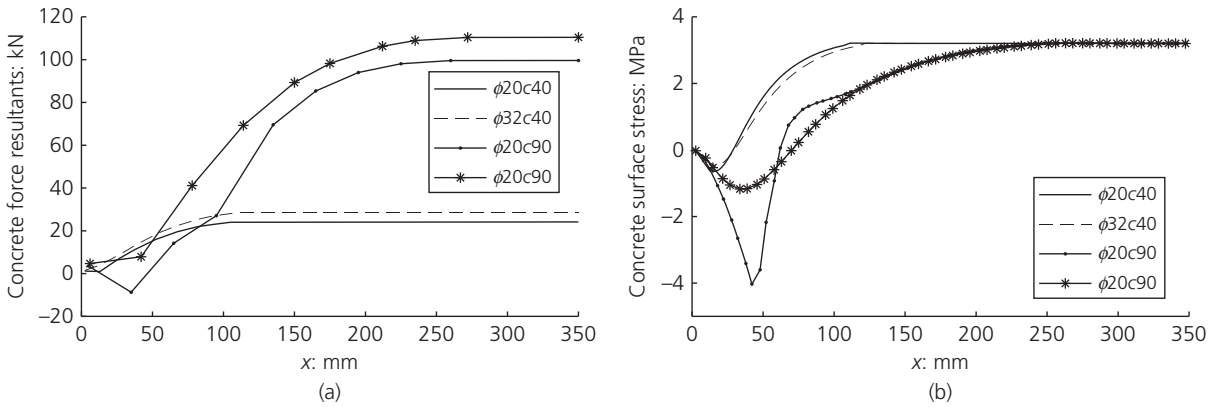

Figure 10. (a) Development of concrete force resultants over the bar length at cracking. (b) Development of concrete surface stresses over the bar length at cracking

of the corresponding concrete surface stresses over the respective transfer lengths.

Although the cover appears to be governing for the crack spacing in virtual experiments, in physical experiments the bar diameter could still have a substantial influence. This can mainly be attributed to the large scatter of the tensile strength of concrete in real-life structures (Barre *et al.*, 2016). The influence of the tensile strength will cause a structure to crack more randomly and not necessarily at the end of the transfer length during the crack formation. The division of the member length due to the random cracking will cause an interaction of the CLLM and CHLM behaviour at which both the cover and the bar diameter together play significant roles for the further development of the crack pattern.

Local bond–slip curve

Determining the local bond–slip curves

The slip distributions for the analysed specimens are approximated by numerically integrating the difference in steel and concrete strains over the bar lengths using the method of Riemann sum as

$$4. \quad s(x) = \int_{x}^{L/2} (\varepsilon_s - \varepsilon_c) \mathrm{d}x \approx \sum_{i \mid x \le x_i \le (L/2)} (\varepsilon_{si} - \varepsilon_{ci}) \Delta x$$

where $s(x)$ is the slip at an arbitrary section x; ε_s is strain at the steel surface; ε_c is strain at the outer concrete surface; x_i is the x-coordinate of integration points adjacent to the steel and outer concrete surface; ε_{si} and ε_{ci} are, respectively, the steel and concrete strains at these integrations points; and Δx is half the FE length.

A 2×2 integration scheme was applied for the FE. Furthermore, using the strains adjacent to the outer concrete surface implies that the slip is composed of two parts: the relative displacement occurring at the interface between concrete and steel due to formation of internally inclined cracks and shear deformations occurring over the cover. This conforms to the definition of slip in accordance with *fib* bulletin number 10 (*fib*, 2000) and Tan *et al.* (2018). Local bond–slip curves are finally obtained by extracting the shear stresses in steel integration points adjacent to the steel bar surface at the location of the evaluated slip.

The local bond–slip curves

Local bond–slip curves at coordinates $x \approx 0$, $x = L/8$, $x = L/4$, $x = 3L/8$ and $x = L/2$ for steel stresses up to 400 MPa have been extracted from all of the analysed specimens in this study and plotted in Figure 11. Both CLLM and CHLM behaviour with specimen lengths corresponding to Figures 6–9 have been included in the plots. Figure 11 shows that the local bond–slip curves in general vary with the geometry of the RC tie. However, there are some significant resemblances. Except for the post-peak region, which occurs at relatively large steel stresses, the local bond–slip curves are seen to exhibit quite similar behaviour independent of the location over the bar length for a given geometry. The exceptions are the local bond–slip curves located in the vicinity of the primary crack ($x \approx 0$) owing to the combined formation of inclined and splitting cracks taking place here, as could be observed in Figure 4(b). This suggests that one local bond–slip curve is sufficient in describing the mean bond transfer for a certain RC tie. Moreover, the bond–slip curve includes the effect that the stiffness reduction of the confining concrete has on reducing the bond transfer due to internal cracking.

The local bond–slip curve proposed by Eligehausen *et al.* (1983) and later adopted by MC2010 (*fib*, 2013)

$$5. \quad \tau = \tau_1 \left(\frac{s}{s_1} \right)^{\alpha}$$

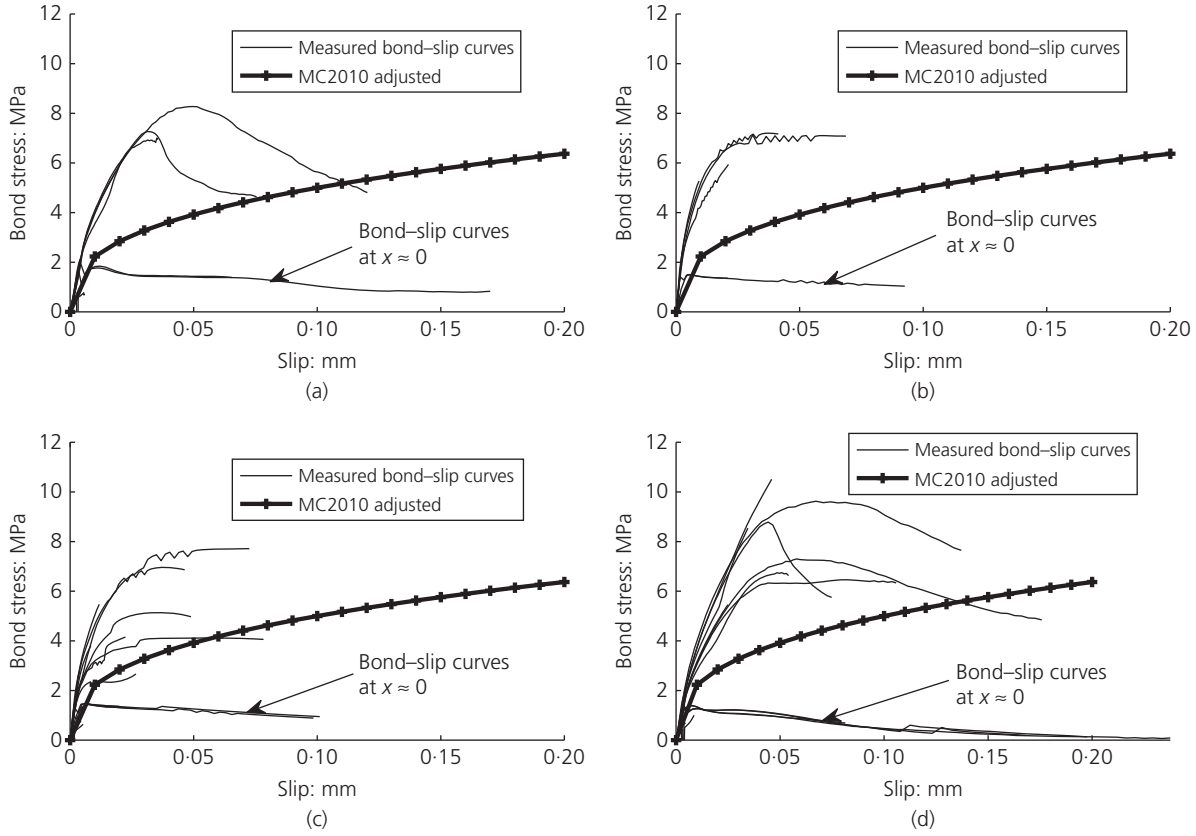

Figure 11. Local bond–slip curves for: (a) the 'Bresler and Bertero' specimens; (b) the 'Yannopoulos' specimens; (c) ϕ20c40 and ϕ32c40; (d) ϕ20c90 and ϕ32c90

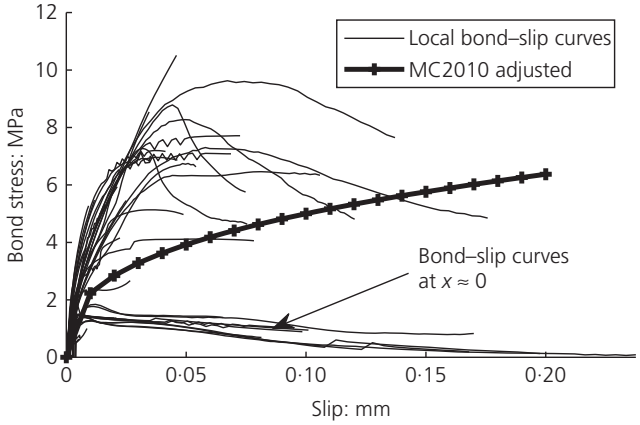

Figure 12. (a) Local bond–slip curves for all of the analysed specimens

is plotted with the parameters $\tau_1 = 5{\cdot}0$ MPa, $s_1 = 0{\cdot}1$ mm and $\alpha = 0{\cdot}35$ in Figure 11, while Figure 12 shows all of the bond–slip curves obtained, plotted together with Equation 5. It is seen that the chosen parameters for Equation 5 tend to serve as a mean for all of the bond–slip curves obtained, irrespective of geometry and location over the bar length. This has an important practical significance in the sense that only one bond–slip curve seems to be necessary in describing the average behaviour of an arbitrary RC tie. Moreover, solving the second order differential equation for the slip using the bond–slip curve in Equation 5 yields an analytical model that is capable of (*i*) replicating the NLFEA conducted in this paper and (*ii*) predicting consistent and conservative crack spacing and crack width. The latter is an approach the authors in this paper currently are developing.

Conclusions

Based on the findings in this study, the following conclusions can be drawn.

- The FE model used to conduct virtual experiments is based on the assumption that the concrete follows the longitudinal displacement field of steel at the interface, which has proven to predict the cracking behaviour of cylindrical RC ties quite accurately.
- Virtual experiments on four different RC ties show that the crack spacing can be proven mechanically to be a geometrically dependent parameter governed by the size

of the cover, and not the bar diameter. In physical experiments, however, the bar diameter could still have a substantial influence. This is due to the large scatter of the tensile strength, which will greatly influence the crack spacing and thus the interaction of the CLLM and CHLM behaviour.

- The cover size does not explicitly increase the crack width by itself, but contributes implicitly by increasing the crack spacing that the steel strains are integrated over. Larger crack spacing simply results in larger crack widths.
- Large bar diameters have a beneficial effect in reducing the steel stresses and the appurtenant steel strains, which in turn reduce the crack widths.
- A local bond–slip curve accounts for the effect that the stiffness reduction of the confining concrete has on the bond transfer due to internal cracking. Moreover, one bond–slip curve is sufficient to describe the average bond behaviour of an RC tie with arbitrary geometry. This has a practical significance that enables an analytical model capable of replicating the NLFEA results.

Acknowledgement

The work presented in this paper is part of an ongoing PhD study funded by the Norwegian Public Roads Administration as a part of the Coastal Highway Route E39 project.

REFERENCES

ACI (American Concrete Institute) Committee (2001) *Control of Cracking in Concrete Structures (ACI 224R-01)*. ACI, Farmington Hills, MI, USA.

Balázs GL (1993) Cracking analysis based on slip and bond stresses. *ACI Materials Journal* **90(4)**: 340–348.

Balázs GL, Bisch P, Borosnyói A *et al.* (2013) Design for SLS according to *fib* Model Code 2010. *Structural Concrete* **14(2)**: 99–123.

Barre F, Bisch P, Chauvel D *et al.* (2016) *Control of Cracking in Reinforced Concrete Structures: Research Project CEOS.fr (Civil Engineering and Geomechanics)*. ISTE Ltd, London, UK.

Base GD, Read JB, Beeby AW and Taylor HPJ (1966) *An Investigation of the Crack Control Characteristics of Various Types of Bar in Reinforced Concrete Beams*. Cement and Concrete Association, London, UK, Research Report 18, Part 1.

Beeby AW (1979) The prediction of crack widths in hardened concrete. *The Structural Engineer* **57A(1)**: 9–17.

Beeby AW (2004) The influence of the parameter ϕ/ρ_{eff} on crack widths. *Structural Concrete* **5(2)**: 71–83.

Belletti B, Damoni C, Hendriks MAN and de Boer A (2014) Analytical and numerical evaluation of the design resistance of reinforced concrete slabs. *Structural Concrete* **15(3)**: 317–330.

Borosnyói A and Snóbli I (2010) Crack width variation within the concrete cover of reinforced concrete members. *Építőanyag – Journal of Silicate Based and Composite Materials* **62(3)**: 70–74.

Bresler B and Bertero VV (1968) Behavior of reinforced concrete under repeated load. *Proceedings of the ASCE – Journal of the Structural Division* **94(6)**: 1567–1590.

Broms BB (1968) Theory of the calculation of crack width and crack spacing in reinforced concrete members. *Cement Och Betong* **1**: 52–64.

Caldentey AP, Peiretti HC, Iribarren JP and Soto AG (2013) Cracking of RC members revisited: influence of cover, $\phi/\rho_{\text{s,ef}}$ and stirrup spacing – an experimental and theoretical study. *Structural Concrete* **14(1)**: 69–78.

CEB (Comité Euro-International du Béton) (1985) *CEB Design Manual on Cracking and Deformations*. École Polytechnique Fédérale du Lausanne, Lausanne, Switzerland.

CEN (European Committee for Standardization) (2004) EN 1992-1-1 Eurocode 2: Design of concrete structures – Part 1-1: General rules and rules for buildings. European Committee for Standardization, Brussels, Belgium.

Debernardi PG and Taliano M (2013) Effect of secondary cracks for cracking analysis of reinforced concrete tie. *ACI Materials Journal* **110(2)**: 209–216.

Debernardi PG and Taliano M (2016) An improvement to Eurocode 2 and *fib* Model Code 2010 methods for calculating crack width in RC structures. *Structural Concrete* **17(3)**: 365–376.

Diana FEA BV (2016) *DIANA Finite Element Analysis User's Manual Release 10.1*. Diana FEA BV, Delft, the Netherlands.

Dörr K (1978) Bond-behaviour of ribbed reinforcement under transversal pressure. *Proceedings of IASS Symposium on Nonlinear Behaviour of Reinforced Concrete Spatial Structures*. Werner Verlag, Düsseldorf, Germany, vol. 1, pp. 13–24.

Eligehausen R, Popov EP and Bertero VV (1983) *Local Bond Stress–Slip Relationships of Deformed Bars under Generalized Excitations*. University of California, Berkeley, CA, USA, Report No. UCB/EERC 83-23.

Feenstra PH (1993) *Computational Aspects of Biaxial Stress in Plain and Reinforced Concrete*. PhD thesis, Delft University of Technology, Delft, the Netherlands.

Ferry-Borges J (1966) *Cracking and Deformability of Reinforced Concrete Beams*. IABSE Publications, Zurich, Switzerland.

fib (International Federation for Structural Concrete) (2000) *Bond of Reinforcement in Concrete – State-of-Art Report*. *fib*, Lausanne, Switzerland, *fib* bulletin no. 10.

fib (2013) *fib Model Code for Concrete Structures 2010*. Wiley, Hoboken, NJ, USA.

Gergely P and Lutz LA (1968) Maximum crack width in reinforced concrete flexural members. In *Causes, Mechanisms and Control of Cracking in Concrete* (Philleo RE (ed.)). American Concrete Institute, Farmington Hills, MI, USA, SP-20, pp. 87–117.

Goto Y (1971) Crack formed in concrete around deformed tension bars. *ACI Journal* **68(4)**: 244–251.

Hendriks MAN, de Boer A and Belletti B (2017) *Guidelines for Nonlinear Finite Element Analysis of Concrete Structures (RTD:1016-1: 2017)*. Rijkswaterstaat Centre for Infrastructure, Utrecht, the Netherlands.

Hordijk DA (1991) *Local Approach to Fatigue of Concrete*. PhD thesis, Delft University of Technology, Delft, the Netherlands.

Husain SI and Ferguson PM (1968) *Flexural Crack Width at the Bars in Reinforced Concrete Beams*. Center for Highway Research, The University of Texas at Austin, Austin, TX, USA, Research Report Number 102-1F.

Jiang DH, Shah SP and Andonian AT (1984) Study of the transfer of tensile forces by bond. *ACI Journal* **81(4)**: 251–259.

Lutz LA (1970) Analysis of stresses in concrete near a reinforcing bar due to bond and transverse cracking. *ACI Journal* **67(10)**: 778–787.

Mirza SM and Houde J (1979) Study of bond stress–slip relationships in reinforced concrete. *ACI Journal* **76(1)**: 19–46.

Nilson AH (1972) Internal measurement of bond slip. *ACI Journal* **69(7)**: 439–441.

Russo G and Romano F (1992) Cracking response of RC members subjected to uniaxial tension. *Journal of Structural Engineering* **118(5)**: 1172–1190.

Saliger R (1936) High-grade steel in reinforced concrete. *Proceedings of the 2nd Congress of the International Association for Bridge and*

Structural Engineering, Berlin-Munich, Germany. ETH, Zürich, Switzerland, pp. 293–315.

Somayaji S and Shah SP (1981) Bond stress versus slip relationship and cracking response of tension members. *ACI Journal* **78(3)**: 217–225.

Tammo K and Thelandersson S (2009) Crack behavior near reinforcing bars in concrete structures. *ACI Structural Journal* **106(3)**: 259–267.

Tammo K, Lundgren K and Thelandersson S (2009) Nonlinear analysis of crack widths in reinforced concrete. *Magazine of Concrete Research* **61(1)**: 23–34, https://doi.org/10.1680/macr.2009.61.1.23.

Tan R, Eileraas K, Opkvitne O *et al.* (2018) Experimental and theoretical investigation of crack width calculation methods for RC ties. *Structural Concrete*, https://doi.org/10.1002/suco.201700237.

Watstein D and Mathey RG (1959) Width of cracks in concrete at the surface of reinforcing steel evaluated by means of tensile bond specimens. *ACI Journal* **56(7)**: 47–56.

Yannopoulos PJ (1989) Variation of concrete crack widths through the concrete cover to reinforcement. *Magazine of Concrete Research* **41(147)**: 63–68, https://doi.org/10.1680/macr.1989.41.147.63.

How can you contribute?

To discuss this paper, please submit up to 500 words to the editor at journals@ice.org.uk. Your contribution will be forwarded to the author(s) for a reply and, if considered appropriate by the editorial board, it will be published as a discussion in a future issue of the journal.